Nonlinear interference effects and ion dynamics in the kinetic theory of Stark broadening of the spectral lines of multicharged ions in a dense plasma

A. V. Anufrienko, A. E. Bulyshev, A. L. Godunov, A. V. Demura,
Yu. K. Zemtsov, V. S. Lisitsa, and A. N. Starostin

Troitskiĭ Institute of Innovational and Thermonuclear Research
(Submitted 6 May 1992; resubmitted 30 September 1992)
Zh. Eksp. Teor. Fiz. **103**, 417–437 (February 1993)

We have investigated the influence of nonlinear interference effects (NIE) and the motion of perturbing plasma particles on the shape of the L_α line. We solved the system of equations for the density matrix in a) the static field of the plasma ions and b) a time-dependent field, modeled by means of molecular dynamics. The calculations were performed for hydrogen-like Ar ions surrounded by Ar and Kr nuclei and protons. We have determined the values of the plasma parameters for which NIE and ion dynamics significantly affect the line shape. We compare our computational results with those of other authors.

1. INTRODUCTION

We have recently[1] developed a kinetic theory of Stark broadening of spectral lines and have demonstrated that it can be applied to a three-level scheme modeling transitions with a forbidden component[2] for helium-like multicharged ions. It was shown, by the density-matrix method[3] and by Keldysh's method of kinetic Green's functions,[4–6] that nonlinear interference effects (NIE), due to level mixing occurring as a result of transitions induced between the levels in the quasistatic microfield of the ions as a result of collisions with electrons (compare Refs. 7 and 8), affect the formation of the emission and rescattering spectra. An important consequence of this approach was that the kinetic equations for the populations of the energy levels were replaced by a system of equations for the full atomic density matrix. After the off-diagonal elements were eliminated, this resulted in the appearance of effective field-dependent collision frequencies[1] and the profile now depended on the character of the level population distribution,[1] i.e., the Stark profiles were no longer universal.[9] These results are essentially a consequence of rejecting the usual assumption made in the theory of Stark broadening that the density matrix of the radiating level is diagonal,[9] and they imply that the broadening processes and the dynamics of the atomic subsystem in the Stark microfield now directly affect one another. For this reason, the starting point of such a theory is, in principle, the calculation of the power (compare Ref. 3) emitted (or absorbed and scattered) by the medium, rather than for the correlation function of the dipole moments.[9]

In the present paper this theory is applied to a real system—the L_α line of a multiply charged hydrogen-like ion in a plasma. Here, on the one hand, the complexity of the real structure of levels and NIE are taken into account, while on the other the deviations from the quasistatic state near the line center, which are connected with fluctuations of the ionic microfield in the plasma, are modeled by the methods of molecular dynamics.[9–24] Due to its fundamental importance the latter question has been under intensive study during the last two decades.[9–25] Here we consider conditions when reabsorption and transfer of radiation can be neglected.

2. BASIC EQUATIONS

According to Ref. 1, the line profile $I(\omega)$, corresponding to a radiative transition to the sublevels α of the upper level with principal quantum number n to sublevels β of the lower level with principal quantum number n', is determined by the relations (compare Refs. 3, 7, and 8)

$$I(\omega)=\frac{1}{I_0}\operatorname{Re}\langle -i\sum_{\alpha\beta\lambda} G^{*}_{\alpha\beta}(\lambda,\omega,\vartheta,\phi)\rho^{(\mu)}_{\alpha\beta}(\lambda,\omega,t)\rangle, \tag{1}$$

$$I_0=\int \operatorname{Re}\langle -i\sum_{\alpha\beta\lambda} G^{*}_{\alpha\beta}(\lambda,\omega,\vartheta,\phi)\rho^{(\mu)}_{\alpha\beta}(\lambda,\omega,t)\rangle d\omega, \tag{2}$$

$$G^{*}_{\alpha\beta}(\lambda,\omega,\vartheta,\phi)=\frac{1}{2\pi}i\omega_{\alpha\beta}\sqrt{\frac{\hbar}{\omega}}\sum_{\nu} D^{1}_{\nu\lambda}(\phi,\vartheta,0)\langle\beta|d_\nu|\alpha\rangle, \tag{3}$$

where ω, ϑ, and ϕ are the frequency and emission angles of a photon with polarization λ in the coordinate system of the emitter; $\omega_{\alpha\beta}$ is the frequency of the transition between the upper sublevel α and the lower sublevel β; the brackets in the formulas (1) and (2) denote averaging over an ensemble of stochastic variables and emission angles of the photon; $D^{1}_{\nu\lambda}(\phi,\vartheta,0)$ are Wigner functions for unit angular momentum (dipole radiation); d_ν are the spherical components of the dipole moment of the emitter; and $G_{\alpha\beta}$ is the matrix element of the Hamiltonian of the interaction of an atomic electron with the quantized electromagnetic field and describes spontaneous emission. We note that the formula (1) for the line profile $I(\omega)$ determines the number of photons and not the relative fraction of the radiation energy per spectral interval, as would be the case if the formula for the power of the radiation emitted by the medium were used directly (see Refs. 1 and 3).

The formulas (1)–(2) contain the reduced off-diagonal element of the density matrix

$$\rho^{(\mu)}_{\alpha\beta}(\lambda,\omega,t)=\rho_{\alpha\beta}(\lambda,\omega,t)\exp[i(\omega-\omega_{\alpha\beta})t], \tag{4}$$

describing spontaneous radiative relaxation and determined from the system of equations

 1063-7761/93/020219-10$10.00

$$i\hbar\dot{\rho}^{(\mu)}_{\alpha\beta}(\lambda,\omega,t)=\hbar[\omega-\omega_{\alpha\beta}-i(\Gamma_\alpha+\Gamma_\beta)/2]\rho^{(\mu)}_{\alpha\beta}(\lambda,\omega,t)$$
$$+\sum_\gamma[V_{\alpha\gamma}(t)\rho^{(\mu)}_{\gamma\beta}(\lambda,\omega,t)-\rho^{(\mu)}_{\alpha\gamma}(\lambda,\omega,t)V_{\gamma\beta}(t)]$$
$$+i\hbar\sum_{\alpha'\beta'}\langle\alpha\beta|\Phi|\alpha'\beta'\rangle\rho^{(\mu)}_{\alpha'\beta'}(\lambda,\omega,t)$$
$$+\sum_\gamma[G_{\alpha\gamma}(\lambda,\omega,\vartheta,\phi)\rho^{(0)}_{\gamma\beta}-\rho^{(0)}_{\alpha\gamma}G^{+}_{\gamma\beta}(\lambda,\omega,\vartheta,\phi)],\quad(5)$$

$$i\hbar\dot{\rho}^{(0)}_{\alpha\beta}=\hbar[\omega_{\alpha\beta}-i(\Gamma_\alpha+\Gamma_\beta)]\rho^{(0)}_{\alpha\beta}$$
$$+\sum_\gamma[V_{\alpha\gamma}(t)\rho^{(0)}_{\gamma\beta}-\rho^{(0)}_{\alpha\gamma}V_{\gamma\beta}(t)]+i\hbar\sum_{\alpha'\beta'}\langle\alpha\beta|\Phi|\alpha'\beta'\rangle\rho^{(0)}_{\alpha'\beta'}+iQ_\alpha\delta_{\alpha\beta}.\quad(6)$$

Here $\rho^{(0)}_{\alpha\beta}$ is the density matrix of the atomic system; Q_α is the incoherent pump (recombination, excitation by electron impact, etc.); and Γ_α and Γ_β are the total natural widths of the upper and lower levels, respectively. The interaction with the time-dependent microfield $V_{\alpha\beta}(T)$ of the ions can be represented in the dipole approximation as

$$V_{\alpha\beta}(t)=-\sum_\nu(-1)^\nu E_\nu(t)\langle\alpha|d_{-\nu}|\beta\rangle,\quad(7)$$

where $E_\nu(t)$ are the spherical components of the intensity vector of the electric microfield of the ions. Collisional mixing in Eqs. (5) and (6) is associated with the operator $\hat{\Phi}$, which in the impact approximation (see Ref. 9) has the following form in the JM representation:

$$\langle\alpha\beta|\hat{\Phi}|\alpha'\beta'\rangle=-N_e\frac{4\pi}{3}\frac{e^4}{\hbar^2}\int\frac{f(v)}{v}dv\int\frac{d\rho}{\rho}\left\{\frac{\delta(\beta\beta')\delta(J_1M_1;J_1'M_1')}{2J_1+1}\right.$$
$$\times\sum_{\gamma_1''J_1''}\langle\gamma_1J_1\|r\|\gamma_1''J_1''\rangle\langle\gamma_1''J_1''\|r\|\gamma_1'J_1'\rangle[A(z_1,z_2)+iB(z_1,z_2)]$$
$$+\frac{\delta(\alpha,\alpha')\delta(J_2M_2,J_2'M_2')}{2J_2+1}\sum_{\gamma_2''J_2''}\langle\gamma_2J_2\|r\|\gamma_2''J_2''\rangle\langle\gamma_2''J_2''\|r\|\gamma_2'J_2'\rangle$$
$$\times[A(-z_1',-z_2')+iB(-z_1',-z_2')]$$
$$-2\sum_\nu(-1)^\nu\frac{C^{J_1M_1}_{J_1'M_1'1\nu}C^{J_2'M_2'}_{J_2M_2,1,-\nu}}{\sqrt{(2J_1+1)(2J_2'+1)}}$$
$$\left.\times\langle\gamma_1J_1\|r\|\gamma_1'J_1'\rangle\langle\gamma_2'J_2'\|r\|\gamma_2J_2\rangle A(z_3,z_4)\right\}.\quad(8)$$

Here

$$z_1=\frac{\varrho}{v}\omega_{\gamma_1J_1,\gamma_1'J_1''},\quad z_2=\frac{\varrho}{v}\omega_{\gamma_1''J_1'',\gamma_1'J_1'},$$
$$z_3=\frac{\varrho}{v}\omega_{\gamma_1J_1,\gamma_1'J_1'},\quad z_4=\frac{\varrho}{v}\omega_{\gamma_2J_2,\gamma_2'J_2'},\quad(9)$$
$$z_1'=\frac{\varrho}{v}\omega_{\gamma_2J_2,\gamma_2''J_2''},\quad z_2'=\frac{\varrho}{v}\omega_{\gamma_2''J_2'',\gamma_2'J_2'},$$

$$C^{JM}_{J_1M_1J_2M_2}=(-1)^{J_1-J_2+M}\sqrt{(2J+1)}\begin{pmatrix}J_1 & J_2 & J\\ M_1 & M_2 & -M\end{pmatrix}\quad(10)$$

are the Wigner $3j$-symbols; $A(z_1,z_2)$ and $B(z_1,z_2)$ are the functions defined on p. 101 of Ref. 9; $f(v)$ is the electron velocity distribution function; N_e is the plasma electron density; $|\gamma_2,J_2,M_2\rangle=|\beta\rangle$, $|\gamma_1,J_1,M_1\rangle=|\alpha\rangle$; and $\omega_{\alpha\beta}=(E_\alpha-E_\beta)/\hbar$ is the frequency corresponding to the transition $\alpha\to\beta$. We assume $Ze^2/\hbar v\ll1$. The curvature of the electron trajectories during scattering by the emitting ion with charge Z can then be neglected. Analysis shows (see Appendix II) that for the parameter values of interest to us the calculation of the matrix elements of $\hat{\Phi}$ in Eq. (8) for the problem of the L_α spectrum agrees quite well with the corresponding results obtained by the strong-coupling method.[26] For the L_α line, generally speaking, the matrices of the systems of equations (5) and (6) in the JM representation are of ranks 16 and 64, respectively. The rank can be reduced by considerations of symmetry (see Appendix I). Detailed expressions for the coefficients in Eqs. (5) and (6) are presented in Ref. 27. Inelastic processes for transitions with $\Delta n\neq0$, which leads to the appearance of an additional contribution to the shift of the line components, were neglected (see Ref. 28).

3. METHODS FOR SOLVING THE TIME-DEPENDENT SYSTEM OF EQUATIONS FOR THE DENSITY MATRIX

Calculations of the L_α line spectrum were performed for a stationary plasma in the quasistatic approximation in the ionic microfield and taking into account the effect of the evolution of this field in time by the method of molecular dynamics (MD).[12–18]

In the molecular dynamics procedure the field of the ions is modeled, as done in Refs. 12–18, by a Debye pair potential with the Debye electronic screening radius. The calculation was performed for quasiparticles (ions) moving in a cube in the μ-model.[11] Elastic or periodic boundary conditions or boundary conditions with an isotropic scattering phase function were imposed on the faces of the cube. Ensembles of 50 and 120 particles were employed in the calculations. This gave an accuracy of $\sim10\%$. As usual, the size of the modeling region was determined from the plasma density being modeled. The trajectory of the system was calculated at times much longer than the correlation time $\tau_c\sim r_0/v_i$, where r_0 is the average distance between the particles and v_i is the average velocity of the perturbing ions with respect to the stationary emitter. Conservation of the total energy of the system was checked during the integration process.

As an intermediate result, the values of the correlation function of the fields at the coordinate origin $\langle E(\tau)E(0)\rangle$ were found as a function of the collisionalty of the plasma. The values were found to be in good agreement with the existing calculations.[12] In addition, the distribution function of the electric microfield was calculated in the obviously static region of the parameters. Taking into account the obvious scaling, these values were close to the corresponding results obtained in Ref. 29. The temporal evolution of the microfield at the coordinate origin also is in good agreement with the results of previous calculations.[14] The systems of

equations (5) and (6) were solved with the help of a finite-difference scheme, which was second-order in time, along the temporal evolutionary trajectory, of the ionic microfield modeled by the molecular-dynamics method. In the process the system (5) was solved immediately for the entire set of frequencies ω, and the result was averaged, after Fourier transforming, with respect to the initial conditions and different realizations of the temporal trajectories of the microfield. In this case the dependence of $\rho^{(0)}(t)$ on the plasma microfield is converted into initital conditions for $\rho^{(\mu)}(t)$.

4. COMPUTATIONAL RESULTS FOR THE L_α LINE PROFILE OF MULTICHARGED IONS IN A DENSE PLASMA

The Hamiltonian of the emitting ion includes the Coulomb interaction and relativistic corrections,[30–33] while the interaction with the microfield of the perturbing ions and the electrons is described by the corresponding terms in Eqs. (5) and (6). Since the field leads to the appearance of an effective collision frequency[1] in the balance equations, the usual method (see, for example, Refs. 32 and 34) does not give a complete description of the contour formation process.

The calculations were performed for hydrogen-like Ar ions in an environment, consisting of Ar and Kr nuclei and protons, with variable composition, density, and temperature. The plasma was assumed to be an equilibrium plasma with a single temperature $T_i = T_e$. The calculations showed that with the appropriate simplifications the computer code reproduces the results of Refs. 13, 15, and 16. In addition, it gives the same results as does solving the system (5) and (6) for a static field for values of the parameters such that the effect of the time dependence of the ionic field is negligible.

We now consider the computational results obtained in the approximation in which the electric field generated by the plasma ions is assumed to be static. Figure 1 displays the profile of the L_α line of an Ar XVIII ion in a fully ionized argon plasma for a fixed value of the ionic field

$$E_0 = 2{,}6031\, ZeN_i^{2/3}, \tag{11}$$

which is the Holtzmark (normal) field strength[9] with ion density $N_i = N_e/Z$. The calculation was performed for an electron density of $N_e = 5\cdot 10^{21}$ cm^{-3} and a temperature of 1 keV. The pump term Q_α in Eq. (6) was assumed to be the same for all states with $n = 2$. The contour in Fig. 1 corresponds to stationary emitting ions, i.e., in order to obtain this profile it is also necessary to average over the velocities, which leads to Doppler line broadening. The peaks 1, 2, 3, and 4 correspond to transitions from the levels $2p_{1/2} \pm 1/2$, $2s_{1/2} \pm 1/2$, $2p_{3/2} \pm 1/2$, and $2p_{3/2} \pm 3/2$, respectively, to the ground state $1s_{1/2} \pm 1/2$. The splitting between the peaks is determined by the position of the $2p_{1/2}$, $2s_{1/2}$, $2p_{3/2} \pm 1/2$, and $2p_{3/2} \pm 3/2$ levels, the position of the last level, which is not shifted by the electric field of the plasma ions, being taken as the zero level: $E(2p_{3/2} \pm 3/2) = 0$, $E(2s_{1/2}) = -4.645$ eV, and $E(2p_{1/2}) = -4.816$ eV. Under these conditions the Stark shift of the $2p_{3/2} \pm 1/2$ level is insignificant, and for this reason the peaks *3* and *4* coincide in the case of the profile for circular polarization ($\Delta M = \pm 1$) (Figs. 1c and d) and averaged over all possible polarizations (Figs. 1e, f, and g). The widths of the peaks *1*, *3*, and *4* are mainly determined by the radiative decay $A(2p_J \to 1s) \approx 0.043$ eV, and the width of the peak 2 is determined by radiative decay and collisions with electrons: $\nu \approx 0.003$ eV.

Figure 1 illustrates the effect of NIE on the line shape. The switching off of the NIE was simulated by equating to zero the off-diagonal elements in the matrix $\rho^{(0)}_{\alpha\beta}$ for different polarizations (Figs. 1a, c, and e). In the case of emission profiles for unpolarized light the switching off of the NIE was likewise simulated by setting to zero the off–diagonal elements of $\rho^{(0)}_{\alpha\beta}$ in Eq. (5) (Fig. 1f). Comparing Fig. 1a (profile of the L_α $\Delta M = 0$ line, neglecting NIE) and Fig. 1b (same profile but taking NIE into account) shows that the effect under consideration redistributes radiation between the peaks: the peaks *1* and *2* are virtually flattened while the height of peak *3* decreases by 20%. In the case of the profile for circular polarization of the photons ($\Delta M = \pm 1$) the effect is even more pronounced (see Fig. 1c—the profile neglecting NIE and Fig. 1d—the profile taking NIE into account): when NIE are "switched on" the peak *2* becomes 1.5 times higher than peak *1*. Peaks *3* and *4* in Figs. 1c and 1d are indistinguishable, since the shift of the levels in the field for these values of the plasma parameters is small. The "field" term under the conditions considered is

$$\begin{aligned} V &= |V(2p_{1/2} \pm 1/2;\ 2s_{1/2} \pm 1/2)| \\ &= (1/\sqrt{2})|V(2p_{3/2} \pm 1/2;\ 2s_{1/2} \pm 1/2)| \\ &= \sqrt{3} e a_0 E_0/Z = 0{,}14 \text{ eV}, \end{aligned} \tag{12}$$

which is comparable to the Lamb shift $\Delta_L = E(2s_{1/2} - 2p_{1/2}) = 0.161$ eV but still much smaller than the fine-structure scale $\Delta_{fs} = \Delta E(2p_{3/2} - 2p_{1/2}) = 4.816$ eV.

The polarization-averaged profile is displayed in Fig. 1e (no NIE), Fig. 1f [with NIE switched off by setting to zero the off-diagonal elements of $\rho^{(0)}_{\alpha\beta}$ in Eq. (5)], and in Fig. 1g (with NIE). Comparing Figs. 1f and 1g illustrates the effect of NIE on the profile. It is manifested as radiation redistribution between the peaks *1* and *2* (they seemingly change places), while the amplitude of the peaks *3* and *4* remains practically unchanged. From the standpoint of terminology, NIE are to be understood as the role of the off-diagonal elements of $\rho^{(0)}_{\alpha\beta}$ in Eq. (5); this role is made clear by comparing Figs. 1f and 1g. Figure 1e was constructed by calculating the populations of the energy levels neglecting the kinetics, which is a very rough approximation for the given values of the plasma parameters. In stronger fields such a calculation is identical to the calculation performed with equally populated levels.

As the field intensifies the levels move apart and radiation is redistributed among the components. For example, for the higher electron density $N_e = 1.43\cdot 10^{23}$ cm^{-3} the $2p_{2/3} \pm 1/2$ level is appreciably shifted from its zero position; the $2p_{1/2}$ level shifts in the opposite direction by approximately the same amount and the $2s_{1/2}$ level approaches its limiting (in the sense $V \gg \Delta_{fs}$) position, equal to $-2\Delta_{fs}/3 = -3.211$ eV. In this case the NIE have virtually no effect on the intensity of the peaks for both linear and circular polarization. Thus, in the case of circular polarization two closely spaced peaks "survive" with increasing electron density: The undisplaced component $2p_{3/2} \pm 3/2 \to 1s_{1/2} \pm 1/2$

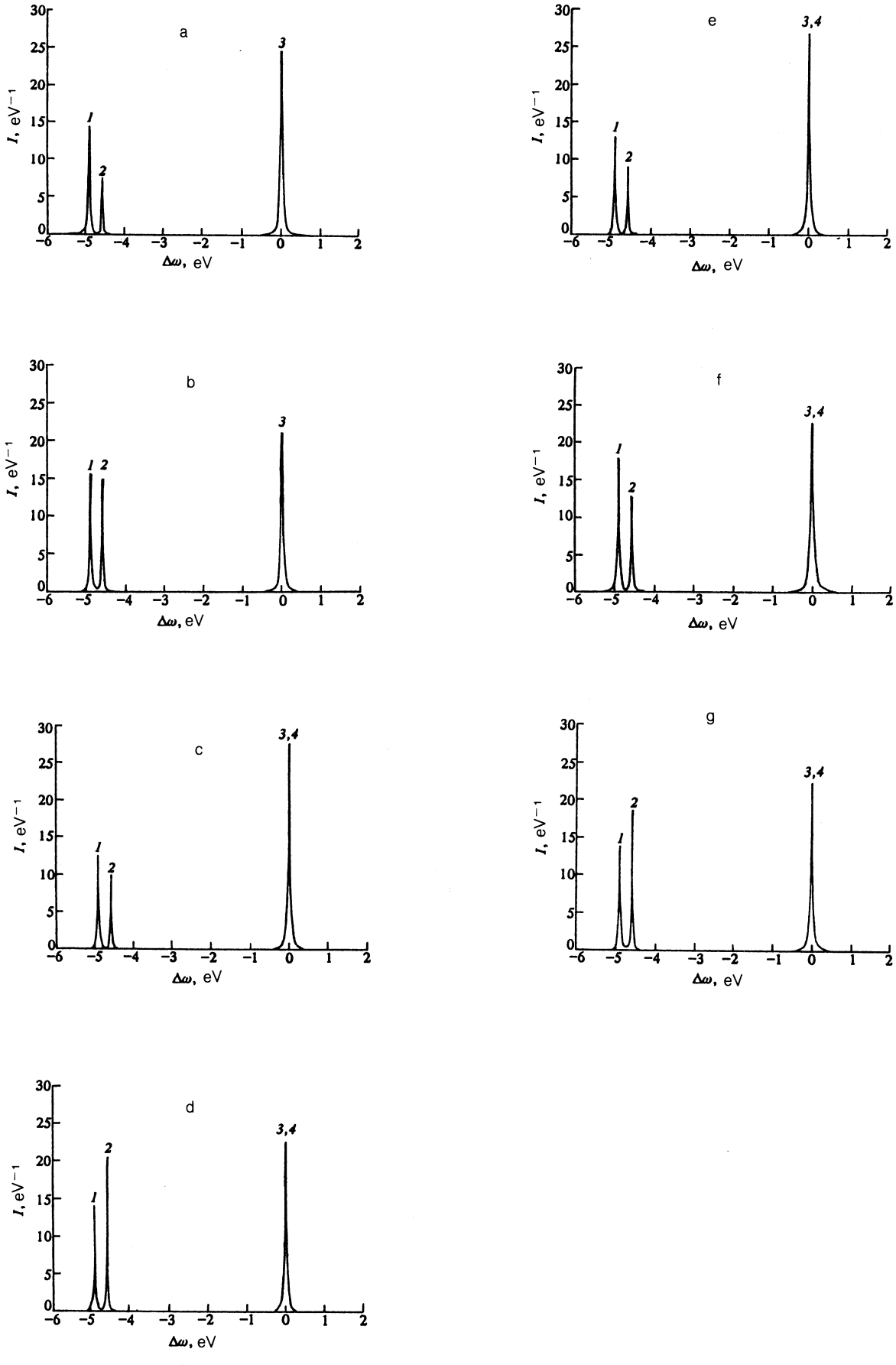

FIG. 1. Profile $I(\omega)$ of the L_α spectral line of an Ar XVIII ion in an argon plasma with a temperature of 1 keV and electron density $5 \cdot 10^{21}$ cm^{-3} before averaging over microfields and velocities for linear polarization without (a) and with (b) NIE, circular polarization without (c) and with (d) NIE, unpolarized radiation without NIE with $\rho_{\alpha\beta}^{(0)} = 0$ in Eq. (6) (e), and unpolarized radiation without NIE with $\rho_{\alpha\beta}^{(0)} \neq 0$ in Eq. (6) and $\rho_{\alpha\beta}^{(0)} = 0$ in Eq. (5) (f), and unpolarized radiation with NIE (g).

with transition energy equal to the "zero" value (with $V=0$) and the component $2s_{1/2}\pm 1/2\rightarrow 1s_{1/2}\pm 1/2$ with frequency corresponding to the asymptotic position of the $2s$ level $-2\Delta_{fs}/3$. However, the components $2p_{1/2}\pm 1/2 \rightarrow 1s_{1/2}\pm 1/2$ and $2p_{3/2}\pm 1/2\rightarrow 1s_{1/2}\pm 1/2$ shift correspondingly to the left and right and at the same time decrease in amplitude.

In the case of linear polarization we note that peak *2* decreases compared with its magnitude in Figs. 1a and b. In the high-density limit, when $V\gg\Delta_{fs}$, this peak disappears completely, and the peaks *1* and *3* become identical and lie on the energy scale at the points $\pm\sqrt{3v}-\Delta_{fs}$, thereby restoring the pattern of splitting of the $\pm 2\pi$ satellites (linear polarization) in the standard "spinless" theory of the Stark effect in parabolic coordinates for the hydrogen atom.[9] As far as the polarization-averaged contour is concerned, for sufficiently high densities the levels become equally populated. At high densities the NIE are insignificant, since the off-diagonal elements $\rho^{(0)}_{\alpha\beta}$ decrease in magnitude with decreasing population difference $\rho^{(0)}_{\beta\beta}-\rho^{(0)}_{\alpha\alpha}$ and the populations of the levels become the same as the density increases.

In contrast to the picture described above, which is correct for a fixed value of the Stark field for the stationary ion, when averaging is performed over the microfields and velocities of the emitting ion the peaks *1* and *2* merge into a single wide line (see Figs. 2–6 below), which masks the NIE-induced redistribution of radiation between the components $2p_{1/2}\rightarrow 1s_{1/2}$ and $2s_{1/2}\rightarrow 1s_{1/2}$; this can be seen clearly by comparing Figs. 1f and 1g.

Figure 2 displays the Ar XVIII L_α line profile averaged over microfields with a Holtzmark distribution and over velocities with a Maxwellian distribution for the conditions $T=1$ keV and $N_e=5\cdot 10^{21}$ cm^{-3}. The dashed line is the profile under the assumption of equally populated $n=2$ levels. In this case the system of equations (6) was not solved; the same diagonal elements of $\rho^{(0)}_{\alpha\beta}$ were substituted into the system (5) and the off-diagonal terms were assumed to be zero: $\rho^{(0)}_{\alpha\beta}=0$ if $\alpha\neq\beta$. The intensities of the left- and right-hand peaks satisfy the "classical" ratio

$$I_L/I_R = 1/2. \tag{13}$$

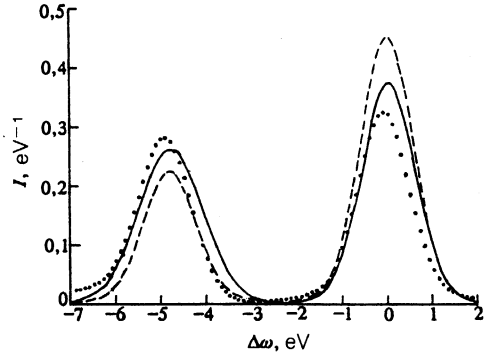

FIG. 2. Profile $I(\omega)$ for an Ar XVIII ion in an argon plasma with a temperature of 1 keV and electron density $5\cdot 10^{21}$ cm^{-3} with averaging over microfields and velocities. The dashed line is the profile calculated in the equal-population approximation, the solid line is the profile obtained taking NIE into account, and the dotted line is the profile calculated by the molecular-dynamics method.

The widths of both peaks are identical and at half-length $\Delta\omega_{1/2}=1.4$ eV, which is somewhat greater than the Doppler half-width $\Delta\omega_D\cdot 2\sqrt{\ln 2}=1.28$ eV, where $\Delta\omega_D=(\omega_0/c)\sqrt{2T/M}$, $\omega_0=3.3$ keV is the L_α transition frequency in Ar XVIII, and M is the ion mass. This is evidently associated with the additional Stark broadening of the levels ($V=0.14$ eV). This profile is identical to the one calculated by the program described in Ref. 33, where broadening of the L_α line of hydrogen-like ions was studied within the conventional approach, based on Fourier transforming the evolution operator, using the wave functions and characteristic energies obtained by solving the secular equation for levels with $n=2$.

The solid line in Fig. 2 is the profile obtained by solving successively the systems (5) and (6). In so doing, the profile corresponding to the solution of the system (5) with off-diagonal elements of the density matrix $\rho^{(0)}_{\alpha\beta}$ ($\alpha\neq\beta$) set artificially to zero (simulation of switching off of NIE) is virtually identical to the profile corresponding to the solution of the system (5) with all $\rho^{(0)}_{\alpha\beta}\neq 0$ (diagonal and off-diagonal) obtained by solving Eq. (6). This illustrates the "washing out" of the NIE as a result of averaging over the microfields and the emitter velocities. The ratio of the peaks in the case of the profile with NIE taken into account is

$$I_L/I_R = 1/1{,}42, \tag{14}$$

i.e., the NIE in the sense indicated (under the conditions considered) do not redistribute the radiation in the peaks after averaging over microfields and velocities. The population redistribution among the levels under the action of the electric field (field-induced mixing) with a simultaneous change in the spontaneous-emission probabilities plays the main role.

Figure 2 also displays the Ar XVIII L_α line profile calculated by the molecular-dynamics method. The dynamics of the broadening ions does not change appreciably the amplitude ratio of the peaks as compared to the quasistatic calculations, but it does change the different line widths somewhat: $(\Delta\omega_{1/2})_L=1.47$ eV and $(\Delta\omega_{1/2})_R=1.38$ eV, whereas in the static case $(\Delta\omega_{1/2})_L=(\Delta\omega_{1/2})_R=1.39$ eV. In addition, both lines undergo a small "red" shift. Finally, some asymmetry appears in the $2s_{1/2}$, $2p_{1/2}$–$1s_{1/2}$ lines. This asymmetry is manifested as an increase in the intensity on the red wing of this line (compare Refs. 35 and 36).

Figure 3 displays the profile of the Ar XVIII L_α line broadened by protons with density $N_p=10^{24}$ cm^{-3} ($N_e=N_p$) and temperature $T=0.862$ keV. The solid curve illustrates the result obtained by solving successively the full systems of equations (5) and (6), i.e., with a Holtzmark microfield distribution; the dashed line was computed using the code of Ref. 33 (under the assumption of equally populated levels) with a Hooper distribution; the dotted line was obtained by the molecular-dynamics method.

It is obvious that taking into account collisions (Hooper distribution) in calculating the static microfield (compare the solid and dotted lines) significantly affects the line shape. It is especially important to take ion dynamics into account in this case, when the broadening particles are light (protons). The most striking manifestation of the ion dynamics is the "washing out" of the dip in the profile be-

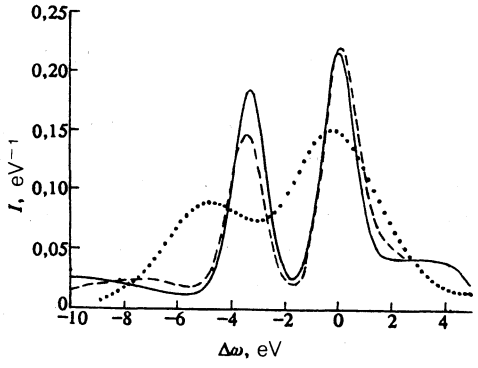

FIG. 3. Profile $I(\omega)$ for an Ar XVIII ion in a hydrogen plasma with a temperature of 0.862 keV and electron density of 10^{24} cm^{-3}. The solid line is the time-independent profile obtained taking NIE into account and with the Holtzmark distribution function for the microfields; the dashed line is the time-independent profile in the equal-population approximation and with the Hooper distribution function; and, the dotted line is the profile calculated by the molecular-dynamics method.

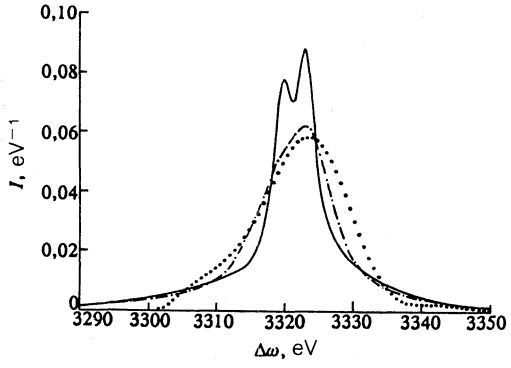

FIG. 5. Profile $I(\omega)$ for an Ar XVIII ion in a hydrogen plasma with a temperature of 0.862 keV and electron density $5 \cdot 10^{24}$ cm^{-3}. The solid line is the time-independent profile presented in Ref. 37; the dot-dashed line is the time-dependent profile from the same work; the dotted line is the time-dependent profile obtained in the present work.

tween the two peaks. We call attention to Refs. 16 and 37, where the profile of the same line, broadened by protons under similar conditions—$N_p = N_e = 10^{24}$ cm^{-3} and $T = 10^7$ K—was calculated by the molecular-dynamics method. The line profile is determined by the evolution operator with diagonalization in the Stark basis for each value of the field (as in Ref. 13).

Note that there is a small discrepancy between the data obtained in Refs. 16 and 37 and our results in both the static case (on the basis of the equal-population assumption[33,37]) and taking ion dynamics into account. The reason for the discrepancy is not entirely clear. In Figs. 4 and 5 our calculations are compared with the calculations performed by the French group[37] for an argon-hydrogen plasma with high densities. In our calculations of the static profile, presented in Fig. 4, the molecular-dynamics distribution function was employed for averaging over the Stark microfields. The series of curves $I(\omega)$ in Figs. 4 and 5 illustrates the qualitative agreement between the results presented. The small discrepancy in the widths and the spectral behavior of the dynamic profiles (see Fig. 5) can be explained by the difference in the approaches used for taking into account the kinetics and by the difference in determining the matrix elements of the operator $\hat{\Phi}$.

The results of similar calculations for the mixture investigated in Ref. 32 (Ar:Kr = 1:1, $T_e = 1$ keV, $N_e = 10^{23}$ cm^{-3}) are presented in Fig. 6. We note that under these conditions the usual approach based on the evolution operator agrees with the results obtained in the present work taking into account NIE and ion dynamics.

CONCLUSIONS

The approach presented in this paper takes into account most fully the kinetics of the atomic subsytem in a fluctuating Stark microfield together with the ion dynamics and "spontaneous" sources appearing in the atomic-photon density matrix due to the off-diagonal elements of the atomic matrix $\rho^{(0)}_{\alpha\beta}$ (NIE). Compared with Ref. 1, where NIE significantly affect the resulting profile of the lines of helium-

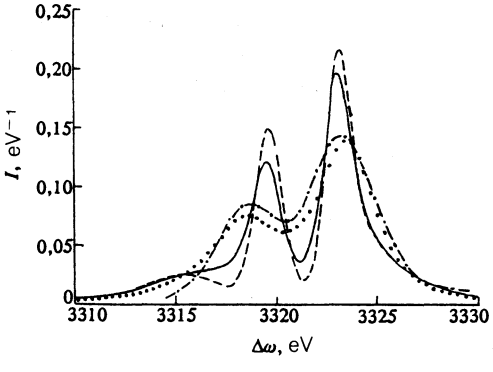

FIG. 4. Profile $I(\omega)$ for an Ar XVIII ion in a hydrogen plasma for the same conditions as in Fig. 3. The dashed curve is our computed time-independent profile; the solid curve is the analogous profile presented in Ref. 37; the dot-dashed curve is the time-dependent profile from the same work (Ref. 37); and, the dotted curve is the time-dependent profile obtained in the present paper.

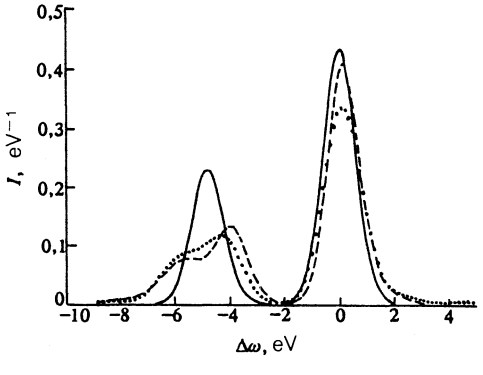

FIG. 6. Profile $I(\omega)$ for an Ar XVIII ion in a krypton plasma with a temperature of 1 keV and electron density of 10^{23} cm^{-3}. The dotted line is the time-dependent profile; the solid line is the time-independent profile taking NIE into account and using the Holtzmark distribution function; the dashed line is the time-independent profile in the equal-population approximation and with the Hooper distribution function.

like ions which contains the contribution of the forbidden component, is found to be significant, NIE play only a small role ($\sim 5\%$) in the average L_α line profile. In this case, in contrast to the usual approach, based on the assumption of equal populations of Stark states, the nonequilibrium nature of the atomic subsystem is more important and it results in significantly different diagonal elements of the atomic density matrix. For low electron densities ($N_e \leqslant 10^{23}$ cm^{-3}) taking ion dynamics into account even in the broadening of the Ar XVIII ion lines by bare argon nuclei gives results which are virtually identical to the static calculations. In both cases, however, the profile obtained is different from the one obtained by calculating the evolution operator.[33,38–40] Ion dynamics are most important in the case of broadening by light hydrogen ions and $N_e \sim 10^{24}$ cm^{-3} and the assumption of equal state populations is found to be justified.

In the light of the discussion presented above, it should be mentioned that we have already pointed out in our previous work[1] the importance of taking into account the effect of NIE on the spectra of multicharged ions and their dielectronic satellites, in view of the fact that the populations of the corresponding levels deviate from their equilibrium values in the presence of NIE. The importance of NIE in this context was confirmed by the results obtained recently in Ref. 34, where it was found that the spectra of the dielectronic satellites of lithium- and helium-like ions are strongly affected by the nonequilibrium population of the corresponding levels which is determined without NIE. Our approach makes it possible to study rigorously and systematically the formation of the spectra of dielectronic satellites of multicharged ions.

In the calculations presented the matrix elements determining the expression for the plasma-electron collision integral do not contain imaginary parts, whose presence in the equations for the density matrix $\rho_{\alpha\beta}^{(\mu)}$ is one of the sources of the shifts of the multiplet components. The influence of this factor, however, can be appreciable[18,28,1)] and will be taken into account in the future together with the nonuniformity of the ionic microfield.[35,36] The matrix elements were calculated in a basis of spherical wave functions, defined in the laboratory coordinate system, and do not depend on time in the process of modeling and solving the system of equations for the density matrix, in contrast to earlier works on ion dynamics (see Refs. 2 and 10) where a basis of "dressed states" in a slowly varying ion microfield was employed.

If exotic conditions are neglected, it can be shown that ion dynamics do not affect significantly the emitter—plasma-electron collision integral.[2,10] However, the collision integral in the equations for the density matrix can become time-dependent in the process of modeling by the molecular dynamics method if the μ model is rejected and microfield fluctuations caused by the motion of the emitter must be taken into account, and this in turn results in the appearance of coupling of Stark broadening and thermal motion.[9,10] In the approach based on the evolution-operator formalism,[13] these effects were found to be insignificant, but they must be analyzed anew on the basis of the kinetic approach.[2)]

In conclusion we thank R. Stamm, B. Talin, F. Khelfaoui, and A. Calisti for providing to us detailed results of their calculations and investigations, which allowed us to compare with our results. We are also grateful to A. Syuro for encouragement.

APPENDIX I

Symmetry relations for the matrix elements of $\rho^{(\mu)}$ and $\rho^{(0)}$

For the L_α line the system of equations (6) for the density matrix $\rho^{(0)}$ contains 64 equations and the system of equations for the matrix $\rho^{(\mu)}$ contains 16 equations [see Eq. (5)]. The calculations for the matrix elements of $\rho^{(0)}$ can be shortened by using the property that the elements of the density matrix are complex conjugates of one another $\rho_{ik}^{*} = \rho_{ki}$ (the diagonal elements are real). The diagonal elements of $\rho^{(0)}$, differing only by the sign of the projections of the angular momenta, are identical:

$$\rho^{(0)}(2lJM;\ 2lJM) = \rho^{(0)}(2lJ - M;\ 2lJ - M). \qquad \text{(AI.1)}$$

This is the consequence of the so-called Kramers degeneracy of energy levels in an electric field.

In addition, in separate cases the number of unknowns can be appreciably reduced by applying the selection rules and the symmetry properties of the off-diagonal elements of $\rho_{ik}^{(0)}$. For example, if the external electric field has a fixed orientation (along the Z axis), then only elements $\rho^{(0)}$ $(2lJM;\ 2l'J'M')$ with the same projections $M = M'$ are nonzero. Then, using Eq. (AI.1) we obtain instead of 64 elements only 20 elements in the matrix $\rho^{(0)}$. Next, using the symmetry properties of the off-diagonal elements of the density matrix $\rho_{ik}^{(0)}$ (discovered in the course of solving the complete system of equations)

$$\begin{aligned}
&\rho^{(0)}(2s_{1/2} - 1/2;\ 2p_{1/2} - 1/2) \\
&\quad = -\rho^{(0)}(2s_{1/2} + 1/2;\ 2p_{1/2} + 1/2), \\
&\rho^{(0)}(2s_{1/2} - 1/2;\ 2p_{3/2} - 1/2) \\
&\quad = \rho^{(0)}(2s_{1/2} + 1/2;\ 2p_{3/2} + 1/2), \\
&\rho^{(0)}(2p_{1/2} - 1/2;\ 2p_{3/2} - 1/2) \\
&\quad = -\rho^{(0)}(2p_{1/2} + 1/2;\ 2p_{3/2} + 1/2),
\end{aligned} \qquad \text{(AI.2)}$$

reduces to 10 the number of unknowns in the system (6).

For linear polarization, when $\nu^{\text{ph}} = 0$, six nonzero elements $\rho^{(\mu)}$ $(2lJM;\ 1s_{1/2}M)$ remain in the matrix $\rho^{(\mu)}$, whose rank is equal to 16; for circular polarization ($\nu^{\text{ph}} = \pm 1$) only four elements remain. In addition, the elements $\rho_{ik}^{(\mu)}$ differing only by the sign of the projections also have a definite symmetry. For example, for $\nu^{\text{ph}} = 0$

$$\begin{aligned}
&\rho^{(\mu)}(2p_{1/2} - 1/2;\ 1s_{1/2} - 1/2) \\
&\quad = -\rho^{(\mu)}(2p_{1/2} + 1/2;\ 1s_{1/2} + 1/2), \\
&\rho^{(\mu)}(2s_{1/2} - 1/2;\ 1s_{1/2} - 1/2) \\
&\quad = \rho^{(\mu)}(2s_{1/2} + 1/2;\ 1s_{1/2} + 1/2), \\
&\rho^{(\mu)}(2p_{3/2} - 1/2;\ 1s_{1/2} - 1/2) \\
&\quad = \rho^{(\mu)}(2p_{3/2} + 1/2;\ 1s_{1/2} + 1/2),
\end{aligned} \qquad \text{(AI.3)}$$

so that the system of equations (5) in this case contains only six unknowns.

APPENDIX II

Relation between the electronic width and the electron-impact excitation cross sections of an ion

We now separate on the right-hand side of Eq. (6) in the collisional term $\Sigma_{\alpha'\beta'}\langle\alpha\beta|\Phi|\alpha'\beta'\rangle\rho^{(0)}_{\alpha'\beta'}$ for the diagonal matrix element of the density matrix $\rho^{(0)}_{\alpha\alpha}\equiv\rho^{(0)}(2lJM;2lJM)$ the terms proportional to the element $\rho^{(0)}_{\alpha\alpha}$:

$$\dot{\rho}^{(0)}(nlJM;\ nlJM) = -N_e\left[\sum_{l'J'}\int\frac{f(v)dv}{v}\frac{4\pi}{3}\frac{e^4}{\hbar^2}\right.$$

$$\left.\times\frac{2}{2J+1}|\langle nlJ\|r\|n'l'J'\rangle|^2\int\frac{d\rho}{\rho}A(Z_{JJ'})\right]\rho^{(0)}(nlJM;\ nlJM). \tag{AII.1}$$

The expression in brackets is the sum of the rates of transitions induced by electron collisions from the level J to the level J':

$$\dot{\rho}^{(0)}(nlJM;\ nlJM) = -N_e\left[\sum_{J'}\langle\sigma(J\to J')v\rangle\right]\rho^{(0)}(nlJM;\ nlJM), \tag{AII.2}$$

where

$$\langle\sigma(J\to J')v\rangle = \int v\sigma(J\to J')f(v)dv$$

$$= \int v\left\{\frac{8\pi}{3}\frac{e^4}{\hbar^2}\frac{1}{v^2}\frac{1}{2J+1}|\langle nlJ\|r\|n'l'J'\rangle|^2\right.$$

$$\left.\times\int\frac{d\rho}{\rho}A(Z_{JJ'})\right\}f(v)dv. \tag{AII.3}$$

In the limit $A(Z)\to 1$ the cross section of the transition $J\to J'$ is

$$\sigma(J\to J') = \frac{8\pi}{3}\frac{e^4}{\hbar^2}\frac{1}{v^2}\frac{1}{2J+1}|\langle nlJ\|r\|n'l'J'\rangle|^2\ln\frac{\rho_{max}}{\rho_{min}}. \tag{AII.4}$$

Introducing the oscillator strength

$$f(J\to J') = \frac{1}{3}\frac{\Delta E}{\mathrm{Ry}}\frac{1}{2J+1}|\langle nlJ\|\frac{r}{a_0}\|n'l'J'\rangle|^2, \tag{AII.5}$$

we obtain

$$\sigma(J\to J') = 8\pi a_0^2\frac{\mathrm{Ry}}{E}\frac{\mathrm{Ry}}{\Delta E}f(J\to J')\ln\frac{\rho_{max}}{\rho_{min}}. \tag{AII.6}$$

Here $E = mv^2/2$ is the electron energy and $\Delta E = E_{J'} - E_J$ is the energy splitting between the levels.

Specifically, for transitions between levels with principal quantum number $n = 2$ we have

$$\sigma(2lJ\to 2l'J') = 12\pi a_0^2\frac{1}{Z^2}\frac{\mathrm{Ry}}{E}(2J'+1)\ln\frac{\rho_{max}}{\rho_{min}}, \tag{AII.7}$$

$$\langle\sigma(2lJ\to 2l'J')v\rangle = 24\sqrt{\pi}a_0^2v_0\frac{(2J'+1)}{Z^2}e^{-\beta}\sqrt{\frac{\mathrm{Ry}}{T}}\overline{\ln\frac{\rho_{max}}{\rho_{min}}}. \tag{AII.8}$$

Here a_0 is the Bohr radius, v_0 is the electron velocity in the first Bohr orbit of the hydrogen atom, and $\beta = \Delta E/T$. Averaging of the velocities is performed for the Maxwellian distribution. The overbar in the last factor in the formula (A II.8) means that the values of $\rho_{\max}$ and $\rho_{\min}$ are taken for the average (thermal) velocity. In the cases of practical interest we have $\beta\ll 1$ (the temperatures at which an ion with charge Z exists are significantly higher than the energy splitting of the fine structure ΔE of the ion) and the exponential in the formula (AII.8) is close to one.

To within a logarithm the formula (AII.6) yields the Bethe cross section for inelastic electronic collisions.[31] In the asymptotic limit, with high collision energies, the argument of the logarithm $\Lambda = \rho_{\max}/\rho_{\min}$ is usually chosen in the form[26]

$$\ln\Lambda^{\text{B-B}} = \ln\left(\frac{1}{\Delta E}\frac{v}{R_0}\right), \tag{AII.9}$$

where R_0 is the interaction radius, which is of the order of the ion size (ΔE, v, and R_0 are given in atomic units). In this case the quantity Λ^{B-B} is determined by the ratio of the period of revolution of a bound electron $1/\Delta E$ to the collision time R_0/v. Here $\rho_{\max} = v/\omega_{JJ'}$, $\rho_{\min} = a_n$, and

$$\Lambda^{\text{B-B}} = \frac{v}{\omega_{JJ'}}\frac{1}{a_n}. \tag{AII.10}$$

We give below expressions for Λ adopted in different approximations often employed for calculating the cross sections for electron-impact excitation of close-lying levels:

a) Bazylev, Chibisov:[41]

$$\lambda^{\text{B-Ch}} = \frac{2}{\gamma}\frac{v}{\omega_{JJ'}}\frac{1}{\rho_c} \tag{AII.11}$$

($\gamma = e^C = 1.78$, $C = 0.5772$ is Euler's constant);

b) Vinogradov, Urnov, Shevel'ko:[42]

$$\Lambda^{\text{V-U-SH}} = \frac{0.7}{a_n}\frac{v}{\omega_{JJ'}} \tag{AII.12}$$

c) Van Regemorter:[43]

$$\Lambda^{\text{V-R}} = \left(\frac{\pi}{\lambda_D}\frac{v}{\omega_{JJ'}}\right)^{1/2}. \tag{AII.13}$$

The formula (AII.6) with the logarithm arguments (AII.10)–(AII.13) exactly reproduces the asymptotic cross sections given in the corresponding works Refs. 41–43. (For low energies the cross sections differ not only by the logarithm.)

We now compare the excitation rates calculated using the formula (AII.8) with the results of calculations recently performed by Zygelman and Dalgarno[26] in the strong-coupling approximation. In this work the cross sections and rates of excitation by electron impact of transitions between fine-structure levels with $n = 2$ were calculated for hydrogen-like ions He II, CV, MgXII, SXIV, and ArXVIII. Table I gives the ratios of the quantities $\langle\sigma v\rangle$ calculated using the

TABLE I. Ratio of transition rates $\langle\sigma v\rangle(\rho_{\min})$ between $n=2$ levels for the Ar XVIII ion calculated from the formula (A.II.8) with different choice of $\rho_{\min}$ to the corresponding quantities $\langle\sigma v\rangle_{ZD}$ from Ref. 26.

T, eV	ρ_{min}				
	ρ^*	$\rho_W^{(4)}$	λ_D	ρ_c	$a_{n=2}$
	Transition $2p_{1/2} \to 2s_{1/2}$				
220	1,02	1,02	1,05	1,11	1,38
441	0,97	0,97	1,03	1,13	1,27
882	0,94	0,94	1,02	1,17	1,19
1763	0,92	0,92	1,02	1,21	1,14
3526	0,92	0,92	1,04	1,25	1,10
7053	0,91	0,91	1,05	1,29	1,08
	Transition $2s_{1/2} \to 2p_{3/2}$				
220	0,85	1,15	0,85	0,97	1,45
441	0,92	1,12	0,92	1,11	1,34
882	0,96	1,09	0,96	1,21	1,25
1763	1,00	1,06	1,00	1,30	1,19
3526	1,04	1,05	1,04	1,38	1,15
7053	1,04	1,04	1,07	1,44	1,11

Note. The upper limit of the impact parameter is $\rho_{\max} = v/\omega_{JJ'}$; $\rho^* = \max(\rho_W^{(4)}, \lambda_D, \rho_c, a_n)$.

formula (AII.8) with different impact parameters $\rho_{\min}$ to the excitation rates $\langle\sigma v\rangle_{ZD}$ from Ref. 26 for the transition $2p_{1/2} \to 2s_{1/2}$ and $2s_{1/2} \to 2p_{3/2}$ in the Ar XVIII ion. The value $\rho_{\max} = v/\omega_{JJ'}$ was used as the upper limit for ρ, since the comparison was made with calculations[26] for an isolated ion (no Debye screening). For this reason, of the two values of the minimum impact parameter $\rho_W^{(2)}$ and $\rho_W^{(4)}$, the Weisskopf radius $\rho_W^{(4)}$ for the quadratic Stark effect was chosen, since the linear Stark effect starts at finite electron densities, when $d_{JJ'}\varepsilon > \Delta E_{JJ'}$, where $\varepsilon \propto N_e^{2/3}$ is the average intensity of the microfields generated by the plasma electrons.

As Table I shows, the formula (AII.8) with the minimum impact parameter (AII.13) on the whole agrees quite well with the calcualtions in the strong-coupling approximation.[26] The average discrepancy is less than 10% (with the exception of the point $T = 220$ eV for the transition $2s_{1/2} \to 2p_{3/2}$). The data in the column for ρ^*, naturally, are identical to the quantities in one of the other columns, i.e., in the column which corresponds to the maximum value of the minimum impact parameter. We note that the choice $\rho_{\min} = \lambda_D$ corresponds, to within a factor of π in the argument of the logarithm, to the van Regemorter approximation (AII.13). However, because the argument of the logarithm contains a square root, the cross section will be two times smaller. To within a factor of $2/\gamma$ in the argument of the logarithm the value $\rho_{\min} = \rho_c$ gives the Bazylev–Chibisov approximation (AII.11); $\rho_{\min} = a_n$ $(n = 2)$ gives the Vinogradov–Urnov–Shevel'ko approximation (AII.12) to within a factor of 0.7. These factors do not change the result significantly, since under the conditions considered the logarithm itself ranges from 6 to 8 for the transition $2p_{1/2} \to 2s_{1/2}$ and from 3 to 6 for the transition $2s_{1/2} \to 2p_{3/2}$. As one can see by comparing the data presented in Table I, the approximations (AII.11) and (AII.12) give reasonable results for the cross sections for inelastic collisions of electrons with an atom, especially since for multiply charged ions collisions become less important as the nuclear charge Z increases than radiative deday: $\langle\sigma v\rangle \propto 1/Z^2$, $A \propto Z^4$. Van Regemorter's approximation differs by approximately a factor of two from the exact calculations for transitions with $\Delta n = 0$.

On the whole the results of Appendix II once again underscore the deep connection, known for a long time in the Born limit[40] and in the Landau–Zener limit[44] and first investigated in Ref. 45 in the intermediate region and in the Stueckelberger antistatic limit, between the line profile in the binary case and the cross section for inelastic transitions.

[1)]H. R. Griem kindly brought this fact to the attention of one of us (A.V.D).

[2)]After this paper was submitted for publication, we completed the molecular-dynamics calculations in which the motion of the emitter was taken into account. The results showed that the motion of the emitter is of little consequence for the plasma conditions considered in this work. We note that the effect of Stark–Doppler coupling[13] was neglected.

[1]A. V. Anufrienko, A. L. Godunov, A. V. Demura *et al.*, Zh. Eksp. Teor. Fiz. **98**, 1304 (1990) [Sov. Phys. JETP **71**, 728 (1990)].
[2]A. J. Barnard, J. Cooper, and E. W. Smith, Quant. Spectrosc. Radiat. Transfer **14**, 1025 (1974).
[3]S. G. Rautian, G. I. Smirnov, and A. I. Shalagin, *Nonlinear Resonances in Atomic and Molecular Spectra* [in Russian], Nauka, Novosibirsk, 1979.
[4]L. V. Keldysh, Zh. Eksp. Teor. Fiz. **47**, 1515 (1964) [Sov. Phys. JETP **20**, 1018 (1964)].
[5]E. M. Lifshitz and L. P. Pitaevskiĭ, *Physical Kinetics*, Pergamon, Oxford, 1981.
[6]A. A. Panteleev, V. A. Roslyakov, A. N. Starostin, and M. D. Taran, Zh. Eksp. Teor. Fiz. **97**, 1777 (1990) [Sov. Phys. JETP **70**, 1003 (1990)].
[7]J. Cooper, Rev. Mod. Phys. **39**, 167 (1967).
[8]J. Cooper, R. J. Ballagh, and I. Hubeny in *Spectral Line Shapes*, edited by J. Szudy, Ossolineum Publ. House, Wroclaw, 1989, Vol. 5, p. 275.
[9]H. Griem, *Spectral Line Broadening by Plasmas*, Academic Press, N. Y., 1974.
[10]A. V. Demura, V. S. Lisitsa, and G. V. Sholin, Zh. Eksp. Teor. Fiz. **73**, 400 (1977) [Sov. Phys. JETP **46**, 209 (1977)].
[11]J. Zeidel in *Spectral Line Shapes*, edited by W. Wende, De Gruyter, Berlin, 1981, Vol. 1, p. 3.
[12]E. L. Pollock and J. C. Weisheit in *Spectral Line Shapes*, edited by F. Rostas, de Gruyter, New York, 1985, Vol. 3, p. 181.
[13]R. Stamm, B. Talin, E. Pollock, and C. Iglesias, Phys. Rev. A **34**, 4144 (1986); *Spectral Line Shapes*, edited by R. J. Exton, Deepak Publ., Hampton, 1987, Vol. 4, p. 141.
[14]E. L. Pollock, *Strongly Coupled Plasma*, World Scientific, New York, 1987, p. 527.
[15]A. Calisti, R. Stamm, and B. Talin, Europhys. Lett. **4**, 1003 (1987).
[16]A. Calisti, F. Khelfaoui, R. Stamm, and B. Talin, *Spectral Line Shapes*, edited by L. Frommhold and J. W. Kato, AIP, New York, 1990, Vol. 6, p. 3.

[17]F. Khelfaoui, A. Calisti, R. Stamm, and B. Talin, *ibid.*, p. 102.
[18]H. F. Griem, M. Blaha, and P. C. Kepple, Phys. Rev. A **41**, 5600 (1990).
[19]D. B. Boercker, C. A. Iglesias, and J. W. Dufty, Phys. Rev. A **36**, 2254 (1987).
[20]D. B. Boercker in *Spectral Line Shapes*, edited by J. Szudy, Ossolineum Publ. House, Wroclaw, 1989, Vol. 5, p. 73.
[21]D. E. Kelleher, D. H. Oza, J. Cooper, and R. L. Greene, J. Quant. Spectrosc. Radiat. Transfer **44**, 101 (1990).
[22]C. Stehle, J. Quant. Spectrosc. Radiat. Transfer **44**, 135 (1990).
[23]E. W. Smith, R. Stamm, and J. Cooper, Phys. Rev. A **30**, 454 (1984).
[24]A. Alastuey, J. L. Lebowitz, and D. Levesque, Phys. Rev. A **43**, 2673 (1991).
[25]S. A. Maiorov, A. N. Tkachev, and S. I. Yakovlenko, Dokl. Akad. Nauk SSSR **229**, 106 (1987); **309**, 1100 (1989) [Sov. Phys. Dokl. **33**, 212 (1988); **34**, 1076 (1989)].
[26]B. Zygelman and A. Dalgarno, Phys. Rev. A **35**, 4085 (1987).
[27]A. V. Anufrienko, A. E. Bulyshev, A. L. Godunov *et al.*, Preprint No. 5514/1, Institute of Atomic Energy, Moscow, 1992.
[28]H. Nguyen, M. Koenig, D. Benredjem *et al.*, Phys. Rev. A **33**, 1279 (1986).
[29]C. F. Hooper, Phys. Rev. **165**, 215 (1968); 169, 193 (1968).
[30]R. D. Cowan, *The Theory of Atomic Structure and Spectra*, University of California Press, Los Angeles, 1981.
[31]L. A. Vainshtein, I. I. Sobel'man, and E. A. Yukov, *Excitation of Atoms and Broadening of Spectral Lines*, Springer, New York, 1981.
[32]R. C. Mancini, D. P. Kilcrease, L. Woltz, and C. F. Hooper, Computer Phys. Commun. **63**, 314 (1991).
[33]E. Kh. Akhmedov, A. L. Godunov, Yu. K. Zemtsov *et al.*, Zh. Eksp. Teor. Fiz. **89**, 470 (1985) [Sov. Phys. JETP **62**, 266 (1985)].
[34]L. A. Woltz, V. L. Jacobs, C. F. Hooper, and R. C. Mancini, Phys. Rev. A **44**, 1281 (1991).
[35]R. F. Joyce, J. A. Woltz, and C. F. Hooper, Phys. Rev. A **35**, 470 (1987).
[36]A. V. Demura, Preprint No. 4632/6, Institute of Atomic Energy, Moscow, 1988.
[37]F. Khelfaoui, "*Modeles de profils Stark d'ions multicharges dans les plasmas chauds*," These, Univ. de Provence, Marseille, 1991.
[38]A. J. Barnard, J. Cooper, and L. J. Schamey, Astron. Astrophys. **1**, 28 (1969).
[39]C. Deutsch, L. Herman, and H. W. Drawin, Phys. Rev. **186**, 204 (1969).
[40]I. I. Sobel'man, *Introduction to the Theory of Atomic Spectra*, Pergamon Press, N.Y., 1977.
[41]V. A. Bazylev and M. I. Chibisov, Usp. Fiz. Nauk **133**, 617 (1981) [Sov. Phys. Usp. **24**, 276 (1981)].
[42]V. P. Shevelko, A. M. Urnov, and A. V. Vinogradov, J. Phys. B **9**, 2859 (1976).
[43]H. van Regemorter, Astrophys. J. **132**, 906 (1962).
[44]A. Jablonski, Phys. Rev. **68**, 78 (1945).
[45]A. V. Demura and V. S. Lisitsa, J. Quant. Spectrosc. Radiat. Transfer **14**, 273 (1974).

Translated by M. E. Alferieff